

## PUPIL LOCALIZATION AND SEGMENTATION USING MORPHOLOGICAL MARKER-CONTROLLED WATERSHED TRANSFORM AND MULTIPLE THRESHOLDING TECHNIQUE

Madhumitha S. and M. Manikandan

Department of Electronics, Madras Institute of Technology, Chennai, India. smadhucool@gmail.com

### ABSTRACT

In this paper, the marker-controlled watershed transform along with morphological operation is proposed to detect the pupil region. Firstly, the contrast enhancement is one to remove the noise caused due to illumination and then morphological reconstruction operations are applied. Standard Open-Close and Standard Close-Open operations are proposed initially, later switched to Close-Open by reconstruction and Open-Close by reconstruction. The experiment is done for 150 images chosen from the CASIA v4 database. Experiment results shows that the Open-Close by reconstruction performed along with watershed transform could detect the complete pupil contour. It also addressed the over-segmentation issue. To segment the pupil region for further analysis Thresholding method is chosen. For various threshold range, the quantitative analysis is performed by evaluating certain features associated with the pupil. The results shows that the Multiple thresholding over the range of 21 pixels yielded better results in terms of accuracy.

*Index Terms* – Morphological operations, Reconstruction, Regional Maxima, Markers, Watershed Transform , Thresholding

### I. INTRODUCTION

In image processing and machine vision learning, it is necessary to obtain accurate position of the pupil as a important characteristic of the human eye [1]. Also among the biometric features, the Biometric with respect to eye is considered more accurate based on a statistic [2]. The pupil segmentation is the initial step for many applications like the iris segmentation system, computer vision system, digital security systems, eye tracking etc [3]. In terms of medical applications, the pupil localization and measurement plays an important role in identifying the abnormalities of the pupillary reactions.

The human eye consists of Sclera, Choroid, Retina, ciliary body, Iris, Pupil, Lens and optic nerves. Iris is a unique feature that have greater stability. Pupil is the opening found inside the iris region to control the amount of light entering the eye. In anatomical terms the aperture in the eye is called as ‘the pupil’ whereas the iris is called as the aperture stop. The pupil is a black circular opening that differs in the size positioned at the center of the iris. Pupil constriction occurs when the size of the pupil is reduced; generally it happens with bright light. When the pupil is enlarged it is said to be dilated. Dilation occurs under dim illumination. The Pupil localization has a wider range of application from face recognition to security access functionalities [4, 5].

Recently there are more researches with respect to pupil localization and segmentation. Bei Yan [6] has formulated a technique in to overcome the influence of various conditions such as luminance, glasses, hair, eyelashes etc while detecting the center of the pupil. A method is proposed to acquire a faster response in pupil detection by Ekteshabi [7]. As a part of the pre-processing the images are decimated by removing the unwanted regions to reduce the computational time. The results are then filtered to remove the noise. In order to split the pupil from the iris and that from the sclera, a thresholding method [8] in conjunction with active contour procedure [9] is chosen.

One major difficulty in pupil detection is the uncontrolled illumination. Retno Supriyanti et al [10] have worked on the images captured under uncon-

trolled illumination using the compact digital cameras. The work presented in this paper uses Edge detection, face detection and the LAB characteristics. Theekapong Charoenpong [11] proposed a method to predict the position of the pupil which is an important parameter for the nystagmus analysis system. The eye image is clicked in a dim environment to protect the subject’s concentrate from other light sources. Initially the pupil is extracted; later the color space conversion is done. An adaptive threshold technique is chosen due to the variation in the illumination.

Mohammed [12] proposed a method to segment the pupil region irrespective of the shape. The light reflections in the pupil region due to illuminators are removed by thresholding. Otsu’s method [13] is used for thresholding, where the threshold value is obtained from the image.

The center of the pupil is detected using a circular Hough transform technique as proposed by Radu et al., [14]. The advantage of the Hough transform technique is that it’s tolerant of gaps in feature boundary descriptions and noise tolerant [15].

In this work, a morphological operation is performed along with the watershed transform to improve the accuracy and over segmentation issue. The morphological operation is done using close, open, erosion and dilation operators. This paper presents four different reconstruction methods and its performance with the watershed transform for pupil detection. After the watershed transform, thresholding technique is chosen to segment out the detected pupil region from the rest of the image for analysis. This method is tested over for 150 eye image samples to evaluate the performance of the reconstruction methods. The results of the watershed transform taken along with the threshold method is used for quantitative analysis.

**II. MARKER BASED WATERSHED SEGMENTATION FOR PUPIL DETECTION:** The marker controlled watershed transform is a type of segmentation algorithm that is in practice because it is robust and is better to segment regions that have closed contour. The main advantage of using this method is that it significantly reduces the amount of over-segmen-

tation. In this method the morphological morphology is used for the marker identification purpose.

The eye images used for pupil segmentation is chosen from CASIA v4 database. The database comprises of more than 30,000 iris images collected from around 1800 genuine sources and 1000 virtual subjects. The images are 8 bit gray level images which are captured under near IR illumination.

**A. Image Enhancement:** To eliminate the noise that is present in the image due to illumination image enhancement is done. The contrast of the image is enhanced in order to retain the important information contained in the image. In the spatial domain the operator acts on the image pixel directly. Intensity adjustment is done by mapping the intensity of the pixels present in the image to a new range of intensities. The image is enhanced, limiting the intensity value of the pixels in the upper bound and lower bound by 1% during the transformation. Using the unsharp masking the image is sharpened. Sharpening the image increases the contrast of the image.

**B. Morphological Processing:** The set of mathematical operations are performed as the pre-processing operation. The watershed algorithm without any pre-processing yields over segmentation. By selecting a proper pre-processing algorithm along with the watershed transform results in more accurate segmentation. In the watershed algorithm, the word watershed refers to a ridge that divides the regions that are immersed by means of various river systems. The region that drains into a river is the Catchment Basin. The Catchment Basin is similar to the watershed of the grayscale image. To obtain a clear difference in the ridges and Catchment basins the pre-processing through morphological operations is done.

**C. Probe Element:** The structuring element must be defined to work along with the morphological operations. The probe or the mask is defined based on the region of interest's geometry. An image is generally the representation of the pixels [16]. Active image is the image that is to be processed, whereas the Probe image is the image that acts as a kernel. The active image is modified by probing it with different structuring elements.

The structuring element defined to detect the pupil region is 'circular disc' shaped. The disc is defined by defining its *d* in pixels. The radius value is chosen as 7 pixel since in the 7 pixel radius maps to the pupil's radius. When there is a mismatch between the active and kernel element it yields in accurate results while performing morphological operations.

**D. Pre-Processing Operations:** The main aim of pre-process is to reduce the over-segmentation effectively. In this work four different morphological approaches are considered. The operations that are studied and analyzed in this work are (1) Close-Open operation (2) Open-Close operation (3) Close-Open by reconstruction and (4) Open-Close by reconstruction. Each of the operation is processed along with the watershed transform to check which method yields robust results.

**E. Standard Reconstruction Process:** The close-open and open-close are called as the standard reconstruction process. The open-close operation is a process in which the morphological erosion is performed later the image is reconstructed from it. In Close-Open process the dilated image is reconstructed with the pre-defined structuring element and finally the image is reconstructed from its complemented image.

**F. Standard Open-Close Operation:** The morphological operation that is initially considered is the Erosion operation. The erosion [17] operation erodes the boundary regions of the foreground pixels. Generally, the white pixels are considered as the foreground pixels. The morphological erosion operation is applied over the database of pupil images.

In general, the erosion of image A by image B, which is given by

$$A \ominus B = \{z \mid B_z \cap A_c \neq \phi\} \quad (1)$$

Where  $\phi$  is the empty set,  $A_c$  is the image to be eroded and  $B_z$  is the structuring element.

Mathematically, Let  $g$  denote the image and  $B$  denote the structuring element as sets in  $Z \times Z$  denoted by

$$(g \ominus B)(x, y) = \min\{g(x + x_i, y + y_i) - B(x_i, y_i) \mid (x + x_i, y + y_i) \in Z, (x_i, y_i) \in Z\} \quad (2)$$

**G. Image Reconstruction:**

The image reconstruction gives clarity to the image the reduces the noise contained in the image. Image reconstruction filters out the connected component which is not a part of the probe element. In standard open-close the eroded image is reconstructed along with the pre-defined structuring element. A point is chosen from the erode image to begin the reconstruction process.

Mathematically, if A is the mask and B is the marker, the reconstruction of B from the image A can be done as an iterative process

1. Initialize a pixel  $h_1$  to be the marker of the image, B
2. Define a structuring element A, generally a 3\*3 matrix consisting of ones
3. Iterate the process

$$h_{i+1} = (h_i \oplus S) \cap A \text{ until } h_{i+1} = h_i \quad (3)$$

Where  $s$  is the structuring element

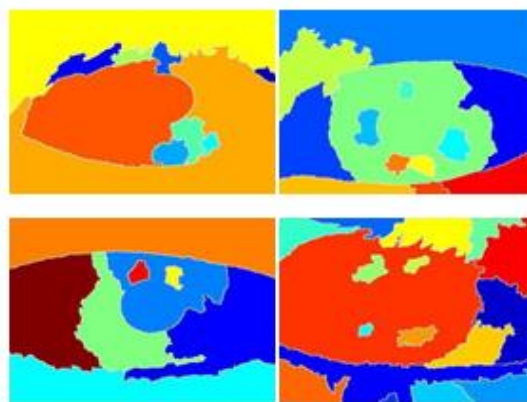


Fig. 1 Results of standard Open-Close applied along with the Watershed Transform

From the results of Standard Open-Close it is found that the pupil contour is not preserved and it also yields to undesirable segmentation results. This method detects the outer contour line but does not detect the central pupil region.

**H. Standard Close-Open Operation:** The dilation operation thickens the object present in the binary image. The dilation of the image A by another image B, which is given by

$$A \oplus B = \{z | B^z \cap A \neq \phi\} \quad (4)$$

where  $\phi$  is the empty set, A is the image to be eroded and  $B_z$  is the structuring element.

Mathematically, when an image g is being dilated by a structuring element B, with g and B as sets in  $Z \times Z$  denoted by

$$(g \oplus B)(x, y) = \max\{g(x - x_1, y - y_1) + B(x_1, y_1) | (x - x_1, y - y_1) \in Z, (x_1, y_1) \in Z\} \quad (5)$$

The image is reconstructed by the same process performed for the standard open-close operation.

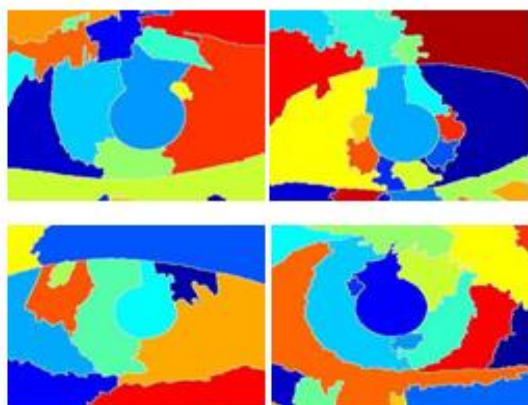


Fig. 2 Results of standard Close-Open applied along with the Watershed Transform

From the results of the Standard close-open operation it is observed that it performs better than the standard open-close operation. This method detects the pupil contour about 80%, but it is unable to detect the complete pupil region. This is due to the erosion and dilation effect on the image.

**I. Open-Close By Reconstruction And Close-Open By Reconstruction**

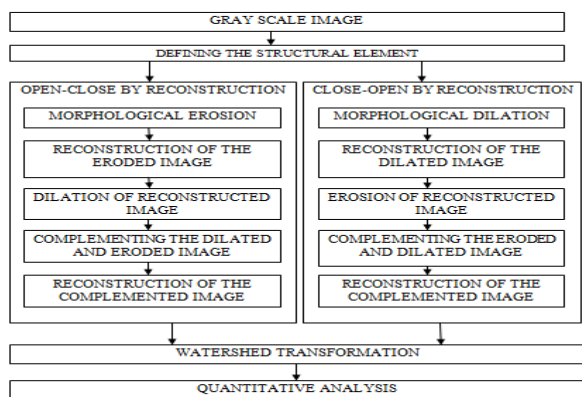


Fig. 3 Workflow of the Open-close and Close-Open Reconstruction process

For this method after defining the structuring element the reconstruction process is done step by step by various morphological operators.

**J. Closing Opening By Reconstruction:** The closing-opening by reconstruction is the process of erosion applied onto the reconstructed dilated image. This process involves the process of dilation, erosion and reconstruction. The same structuring element is used for all the operators. Finally in the closing-opening by reconstruction process the eroded image is again reconstructed. The process of reconstruction is done on the complemented image. The final image obtained undergoes the watershed transform to segment out the pupil region.

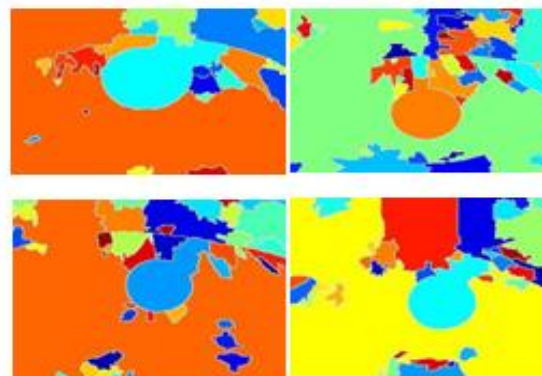


Fig. 4 Results of standard Close-Open by reconstruction applied along with the Watershed Transform

From the images obtained as a result of Closing Opening by reconstruction it is seen that the closed contour of the pupil is not detected. This method performs better compared to the standard reconstruction methods.

**K. Opening Closing By Reconstruction:** The opening-closing is the reverse operation of the close-open reconstruction. In this method the image which is being reconstructed after erosion is considered instead of the reconstructed dilated image. The inputs that are fed to the reconstruction operation are the complemented images of the reconstructed eroded image and the image that is being dilated over the reconstructed eroded image.

Reconstruction-based opening and closing are more effective than standard opening and closing at removing small blemishes without affecting the overall shapes of the objects.

In order to smoothen the image g by the structuring element B is defined mathematically as

$$R(g) = \beta(\theta_l, (g \oplus B)), 0 \leq l \leq n \quad (6)$$

where  $\theta(g)$  is the closing operation,  $\beta$  is the reconstruction operator,  $\theta_l$  is the image reference that is obtained by closing the image g by l times, n is the size of the structuring element B and  $R(g)$  is the smoothening function.

**L. Superimposition Of Regional Maxima:** The opening-closing reconstructed image is chosen to compute the regional maxima. Regional maxima are the connected component pixels having a constant intensity value, t, whose external boundary pixels have

values that are less than  $t$ . The pixels that have the value 1 are identified as regional maxima. The rest of the pixels are set to the value 0. After the regional maxima processing, it is superimposed.

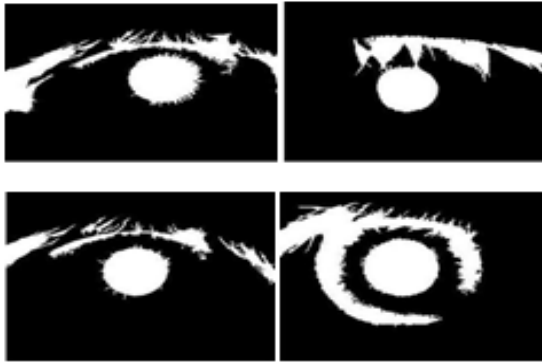


Fig.5 Superimposition of regional maxima

**M. Background Markers:** Generally, the watershed segmentation using markers extracts the seeds that specify the presence of objects or background at specific image locations [18,19]. The background pixels are in black, but it is not preferred the background markers to be too close to the edges of the objects to be segmented. Generally, to overcome this issue the background is thinned by finding the SKIZ i.e., Skeleton by influence zones of the foreground image.

**N. Watershed Transform:** The topographical distance is computed by the Euclidean algorithm between two pixels considering the shortest path.

$$TD(A, B) = f(q) - f(p) \quad (7)$$

The watershed line is a function i.e., the set of points of the function  $f$  which do not belong to any other catchment basin:

$$Wsh(f) = s(f) \cap \left[ \bigcup_i (CB(m_i)) \right]^c \quad (8)$$

where  $s(f)$  is the support to the function  $f$ ,  $CB(m_i)$  is the catchment basin with the regional minima  $m_i$ . After the watershed ridge lines are computed the intensity of the image is modified using morphological reconstruction so that it has the regional minima in the desired locations. The watershed image is computed over the intensity varied images.

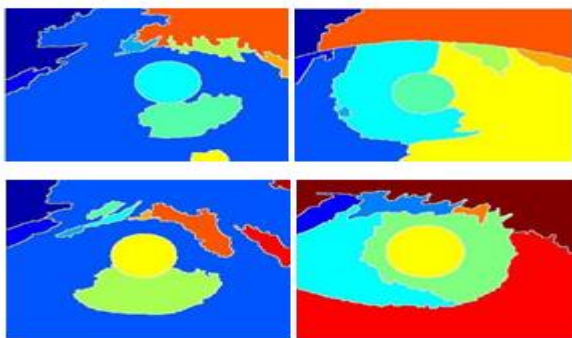


Fig. 6 Results of standard Open-Close by reconstruction applied along with the Watershed Transform

The results of the Open close reconstruction as a pre-processing for the Watershed Transform is shown above. The result is visualized by superimposing the

foreground markers, background markers and the segmented object boundaries on the original image. It is seen that the pupil region of the eye is detected precisely. It is seen that the pupil region has different colors in the image, this distribution is based on the number of segments in each image. The pupil contour is well preserved from the other regions of the eye. Taking the overall image the over-segmentation issue is also well addressed.

### III. QUANTITATIVE ANALYSIS

To perform the quantitative analysis 150 samples were chosen from the CASIA v4 database. The images were chosen with different illumination and interferences factor. The results of the watershed transformed images are in RGB color scale. To begin with the process to extract the feature the image is converted to gray scale. For the gray scale image the histogram is computed to find the maximum repetitive intensity pixel present in the image.

**A. Thresholding Process:** From the histogram, the pixel intensity that has frequent occurrence is chosen as the threshold value. In this work single thresholding and multiple thresholding are performed for quantitative analysis and comparison.

These images are segmented out from the original CASIA v4 database image to obtain the pupil region with its original characteristics. In the image the pupil region is clearly segmented out from the eye image and boundaries are well preserved. These images are used as the base for further comparison.

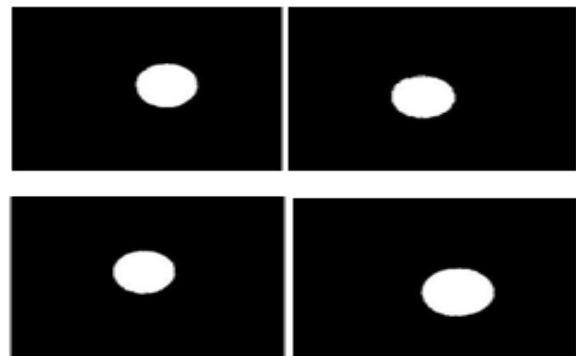


Fig. 7 The pupil region segmented out from the original CASIA v4 database

**B. Single Thresholding:** The maximum frequency intensity is chosen as the threshold value for Single thresholding technique. The pixel value that map with the threshold value is set to a binary value of 0 whereas the other pixels are set to binary 1.

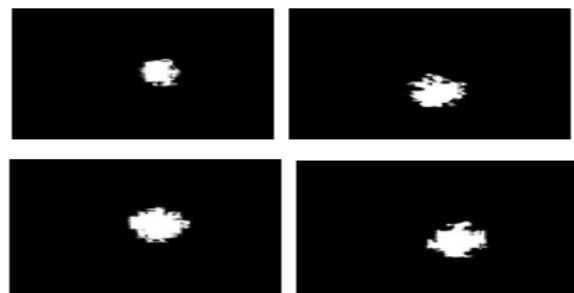


Fig. 8 The pupil region segmentation using Single Threshold Method

**C. Multiple Thresholding:** Extending the threshold value on both the ends equally leads to set of threshold value. This set of values are ranged as  $\pm 2$ ,  $\pm 5$  and  $\pm 10$ . Each range varies over the number of pixels considered for the thresholding process.

For the process of multiple threshold, Initially, the value of threshold is increased to a range of  $\pm 2$ . The range of intensity is over 5 valued intensity pixels.

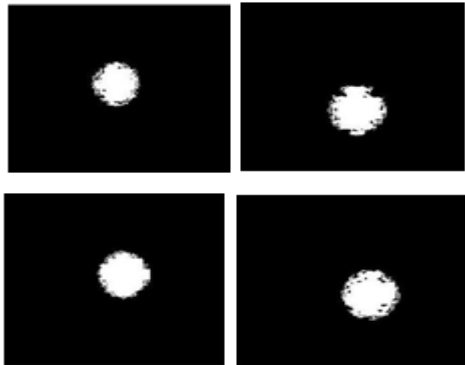


Fig. 9 The pupil region segmentation using Multiple Threshold Method with threshold value of  $\pm 2$

It is seen in the above images that the segmented image consists of certain regions which are not a part of the pupil region. And the pupil region appears better compared to the single threshold value. Next, the range is increased to  $\pm 5$ . It ranges between 11 value.

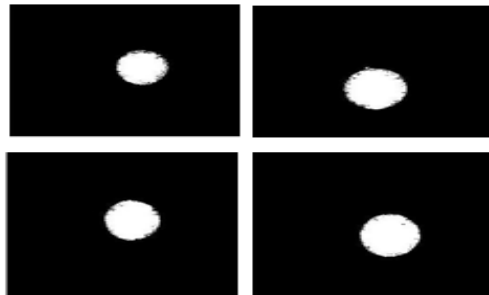


Fig. 10 The pupil region segmentation using Multiple Threshold Method with threshold value of  $\pm 5$

The images that are obtained for the threshold value of  $\pm 10$  are presented.

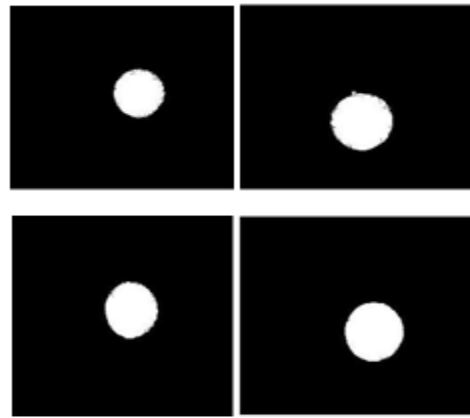


Fig. 11 The pupil region segmentation using Multiple Threshold Method with threshold value of  $\pm 10$

It is found that the threshold value for the range of  $\pm 10$  was closer to the circular geometry. Added to that it has a much well defined boundaries compared to the previous thresholding ranges. 90-95% of the pupil region is preserved in this thresholding range. Increasing the threshold values above this range added to the over-segmentation issue. It would add regions that are outside the boundary, i.e; which do not belong to the region of interest.

#### IV. RESULTS AND DISCUSSIONS

The pupil region that is obtained as a result of watershed transform and multiple thresholding are compared to check the accuracy factor. The parameters considered for comparison are Area, Perimeter, Diameter and roundness.

Perimeter is also called as circumference. The perimeter is the distance around the boundary. The perimeter is computed by calculating the amount of distance between each adjoining pair of pixels around the border region.

Diameter is the distance across circle passing through the center. The diameter of the pupil is calculated by  $\sqrt{(4 * Area)/\pi}$ .

Roundness represents the geometric closeness of the figure to the circle. Roundness scales from 0 to 1.1 represents a perfect circle. The roundness is calculated by  $\frac{4 * \pi * Area}{(Perimeter)^2}$

TABLE I. PERIMETER ACCURACY COMPARISON OF THRESHOLDING METHODS

S.No	Original Perimeter	Single thresholding Perimeter	Multiple thresholding $\pm 2$	Multiple thresholding $\pm 5$	Multiple thresholding $\pm 10$
1	334.04	480.75	596.28	420.31	345.61
2	252.1	245.82	472.94	319.11	269.91
3	251.13	330.49	372.03	311.74	249.74
4	225.62	443.54	416.55	306.19	237.86
5	259.27	375.11	477.87	333.16	268.49
6	267.62	430.57	517.741	353.78	276.29
7	270.45	477.58	505.95	338.86	288.04
8	307.66	461.44	532.58	384.75	310.53
9	243.03	361.66	477.52	294.73	241.37
10	294.14	447.93	506.44	403.62	298.04

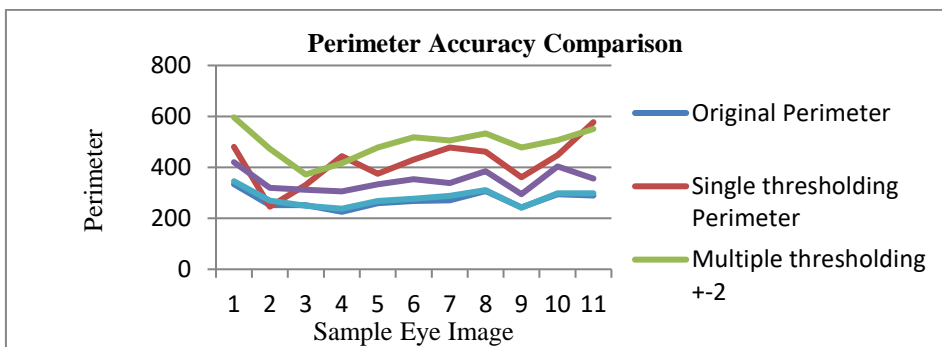


Fig. 12 Accuracy comparison Graph of the pupil perimeter

Perimeter is the continuous line forming the boundary of a closed geometrical figure. The single thresholding method and using the threshold of  $\pm 2$  did not yield accurate results. The former showed up more perimeter while latter resulted in less perimeter.  $\pm 10$  threshold yielded better results close to the original perimeter.

TABLE II. ROUNDNESS ACCURACY COMPARISON OF THRESHOLDING METHODS

S No	Original Roundness	Single Thresholding Roundness	Multiple Thresholding $\pm 2$	Multiple Thresholding $\pm 5$	Multiple Thresholding $\pm 10$
1	0.8948	0.1686	0.2044	0.432	0.8495
2	0.8877	0.2226	0.2052	0.4141	0.9077
3	0.8848	0.109	0.1776	0.3773	0.8951
4	0.8383	0.2256	0.2022	0.4677	0.8554
5	0.8319	0.1795	0.2228	0.3753	0.8162
6	0.8298	0.2631	0.2134	0.4832	0.8121
7	0.8206	0.1424	0.1254	0.5745	0.7723
8	0.8037	0.2016	0.2614	0.4121	0.7973
9	0.7422	0.2113	0.2096	0.3665	0.7034
10	0.7335	0.2166	0.2144	0.4418	0.7446

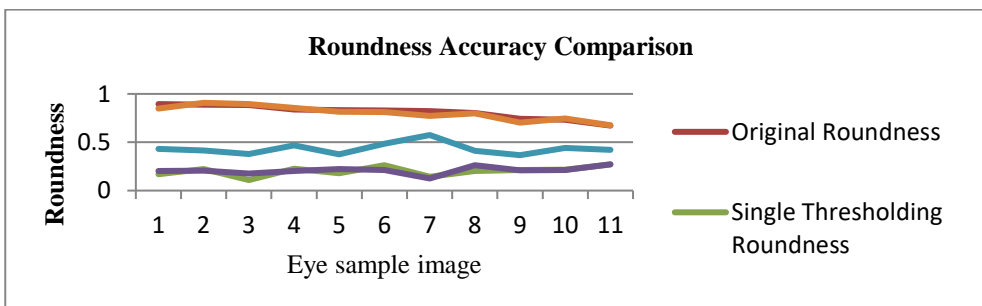


Fig. 13 Accuracy comparison Graph of the pupil Roundness

From the information in Table 2 it can be understood that the Multiple thresholding with  $\pm 10$  threshold yielded result close to the original roundness of the pupil.

The performance of single thresholding and multiple thresholding with  $\pm 2$  is poor. Since the  $\pm 10$  threshold captured the boundary region well, the roundness information is well preserved.

TABLE III. DIAMETER ACCURACY COMPARISON OF THRESHOLDING METHODS

S No	Original Diameter	Single thresholding Diameter	Multiple thresholding $\pm 2$	Multiple thresholding $\pm 5$	Multiple thresholding $\pm 10$
1	65.78	46.91	59.72	63.17	64.26
2	65.53	54.71	61.71	64.29	65.26
3	63.85	45.65	55.99	60.63	62.36
4	63.61	44.63	56.14	60.4	62.57
5	63.05	41.29	56.45	62.35	61.74
6	62.81	46.41	56.23	59.68	61.52
7	62.73	41.15	55.2	59.79	61.51
8	62.29	42.81	56.45	60.29	61.62
9	61.96	42.93	53.74	58.66	60.51
10	61.4	41.52	54.43	58.39	59.56

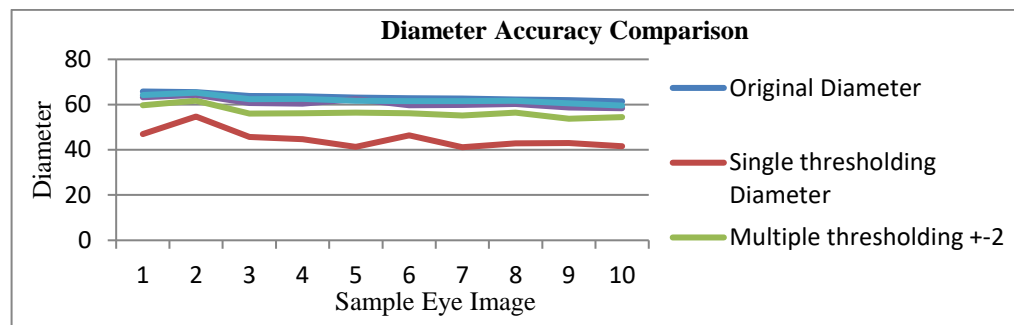


Fig. 14 Accuracy comparison Graph of the pupil Diameter

The diameter single thresholding method is the lowest compared to the other method. Multiple thresholding method  $\pm 2$ ,  $\pm 5$  and  $\pm 10$  yielded closer results to the original. Comparing the multiple thresholding method,  $\pm 10$  yielded diameter close to the original pupil diameter.

#### V. CONCLUSION

The watershed transform is performed along with suitable morphological operation to reduce the over-segmentation issue. The thresholding method was adapted to segment out the pupil region by fixing the threshold. The quantitative analysis is done based on the features like Perimeter, Roundness and Diameter. The single threshold performance was limited since its completely dependent on one intensity pixel in the entire image. Increasing the range of intensities by adding the threshold value equally to both the bounds helped to obtain better results. From the feature extraction comparison it is seen that the Watershed segmentation along with the multiple thresholding with the value of  $\pm 10$  yielded accurate results compared to the other methods. Increasing the threshold further than  $\pm 10$  resulted in over segmentation.

#### REFERENCE

- [1] Vater, Sebastian, and Fernando Puente León, Combining isophote and cascade classifier information for precise pupil localization, Image Processing (ICIP), IEEE International Conference (2016).
- [2] Wang, Y., Y. Zhu and T. Tan, Biometrics personal identification based on iris pattern. Acta Automatica Sinica 28(1): 1-10 (2002).
- [3] F. Song, X. Tan, S. Chen and Z.H. Zhou, A literature survey on robust and efficient eye localization in real life scenarios. J. Pattern Recognition 46(12): 3157–3173 (2013).
- [4] Bastos, Carlos A.C.M., et al., Pupil segmentation using pulling & pushing and BSOM neural network., Systems, Man, and Cybernetics (SMC), IEEE International Conference (2012).
- [5] Valenti, R., N. Sebe and T. Gevers, Combining head pose and eye location information for gaze estimation. IEEE Trans. Image Process 21(2): 802–815 (2012).
- [6] Yan, Bei, et al., A robust algorithm for pupil center detection., 6<sup>th</sup> IEEE Conference on Industrial Electronics and Applications (2011).
- [7] Ektesabi, A. and A. Kapoor, Exact pupil and iris boundary detection, Control, Instrumentation and Automation (ICCIA), 2<sup>nd</sup> International Conference on. IEEE (2011).
- [8] D. A. Chernyak, Iris-based cyclotorsional image alignment method for wavefront registration. IEEE Transactions on Biomedical Engineering 52: 2032-2040 (2005).
- [9] Jomier, J. et al., Automatic quantification of pupil dilation under stress, International Symposium on Biomedical Imaging: Nano to Macro (2004).
- [10] Supriyanti, Retno, et al., Detecting Pupil and Iris under Uncontrolled Illumination using Fixed-Hough Circle Transform. International Journal of Signal Processing, Image Processing and Pattern Recognition (IJSIP) 5(4): 175-188 (2012):
- [11] Charoenpong, Theekapun, et al., Accurate pupil extraction algorithm by using integrated method." Knowledge and Smart Technology, 5<sup>th</sup> International Conference on. IEEE (2013).
- [12] Mohammed Abdullah, A.M., S.S. Dlay and W. L. Woo, Fast and Accurate Pupil Isolation Based on Morphology and Active Contour. International Journal of Information and Electronics Engineering 4(6): 418 (2014):
- [13] Otsu, N., A Threshold Selection Method from Gray-Level Histograms, IEEE Transactions on Systems, Man and Cybernetics 9: 62-66 (1979).
- [14] Bozomitu, Radu Gabriel, et al., Pupil centre coordinates detection using the circular Hough transform technique, 38<sup>th</sup> International Spring Seminar on Electronics Technology (ISSE). IEEE (2015).
- [15] Cherabit, Nouredine, Fatma Zohra Chelali and Amar Djeradi, Circular hough transform for iris localization. Science and Technology 2(5): 114-121 (2012).
- [16] Pandey, Saurabh, Study and implementation of morphology for image segmentation. Diss. Thapar University Patiala (2010).
- [17] Han, Baoan, Watershed Segmentation Algorithm Based on Morphological Gradient Reconstruction. Information Science and Control Engineering (ICISCE), 2<sup>nd</sup> International Conference on. IEEE (2015).
- [18] Avinash, S., K. Manjunath and S. Senthil Kumar, An improved image processing analysis for the

detection of lung cancer using Gabor filters and watershed segmentation technique. In: Inventive Computation Technologies (ICICT), International Conference on IEEE Vol. 3, (2016).

[19] Ravi and AM Khan, Bio-medical Image Segmentation Using Marker Controlled Watershed Algorithm: a case study: International. Journal of Research in Engineering and Technology 3 Special Issue (3): (2014).